Power Disturbance Analysis via Discrete Wavelet Transform

Chau-Shing Wang
Department of Electrical Engineering
National Changhua University of Education
Changhua, Taiwan
Phone: 886-4-723-2105 ex 8212
cswang@cc.ncue.edu.tw

Abstract: - Electric *power quality* is an aspect of power engineering that has been with us since the inception of power systems. To investigate this issue, engineers have proposed various schemes to deal with the power disturbance waveforms. Among these approaches, *wavelet transform* is one of the most frequently used algorithms to analyze the power signal. This paper presents a new design of discrete wavelet transform suitable for *DSP*-based implementation. This approach has the advantages of low cost, real-time calculation, and possible hand-held device implementation. In addition, the experimental results demonstrate accurate disturbance time localization and clear decomposition of power disturbance signals.

Key-words: DSP, wavelet transform, power quality

1. Introduction

In modern electrical power systems, the regularity of power voltage and current is greatly affected by the increasing numbers of nonlinear loads connected in the power grid. Especially, power electronic-based systems such as inverters for driving motors, electronic ballasts, and capacitor switching are the sources causing power quality issues. Power disturbances encountered commonly include power interrupt, sag, swell, transient oscillation, flicker, and harmonic distortion. Capturing and analyzing these power disturbances are essential tasks of monitoring power quality.

In general, power disturbances can be categorized as stationary or non-stationary signals according to their periodicity. The stationary signals, e.g. harmonics and voltage flicker, are typically analyzed by Fourier transform or FFT algorithm. Practical measurements using FFT algorithm assume infinite periodicity of the signal to be transformed. Furthermore, the time-domain information in the signal would be spread out on the whole frequency axis and become unobservable following the transformation. Therefore, this manner alone is not suitable for analyzing non-stationary signals [1]. A modification to the Fourier transform, called short-time Fourier transform (STFT), uses a time-frequency window to localize transients. If the STFT uses a wide time window, then the transient frequencies can be well distinguished by the high resolution of the spectrum domain while the transient locations are not resolvable. As the time window gets smaller, the transient locations become clear while the frequency resolution progressively worsens. Therefore, to localize the transient precisely, we must compute the STFT every time we change the window size, leading to a serious issue of computation load [2].

Wavelet transform has advantages over FFT and STFT for the analysis of signals with transients. Wavelet transform is based on the decomposition of signals according to a set of adaptable scaled and shifted wavelets. This manner of analysis is generally

termed 'multiresolution analysis'. The wavelet transform expands signals not in terms of sine or cosine functions but by wavelets, generated using the translation and dilation of a mother wavelet [3,4].

Over the last years numerous approaches to power quality automatic detection and classification have been suggested [5-9]. However, due to the difficulty in realizing the wavelet transform on a microchip with low-level coding language, most of the studies regarding the wavelet transform are implemented on a PC-based hardware structure with commercial application software, such as MATLAB. Fortunately, Huang et al. [10] successfully accomplished the FPGA realization of wavelet transform for power disturbance detection. Furthermore, Sarkar and Sengupta [11] employed a digital signal processor (DSP) to implement wavelet transform for power factor measurement.

Table 1 Comparison of common used wavelets

	Haar	Daubechies-N	Symmlets	Coiflets	Meyer	Gaussian	Mexican hat	Morlet
DWT	yes	yes	yes	yes	yes (IIR)	no	no	no
CWT	yes	yes	yes	yes	yes	yes	yes	yes
ψ Compact supported	yes	yes	yes	yes	no	no	no	no
Support width	1	2N-1	2N-1	6N-1	∞	∞	∞	∞
Filter length	2	2N	2N	6N	IIR	IIR	IIR	IIR
Orthogonal	yes	yes	yes	yes	yes	no	no	no
Scaling function φ	exist	exist	exist	exist	exist	N/A	N/A	N/A
Reconstruction	yes	yes	yes	yes	no	no	no	no
Fast algorithm	yes	yes	yes	yes	no	no	no	no

This paper provides a new design and deep discussion of discrete wavelet transform (DWT) applied to analyzing power quality events. Moreover, in order to reduce the implementation cost, achieve real-time calculation, and enhance the potential implementation of a hand-held device for this work, the DWT is implemented with Texas Instruments (TI) 32-bit TMS320C6711 DSP along with the TLC320AD535 16-bit analog to digital converter. The experimental results show that the DSP-based implementation of the DWT can accurately detect power transients.

2. Wavelet Theory

A main feature of wavelets is the oscillating and rapid decay to zero. Generally, smooth wavelets indicate higher frequency resolution than wavelets with sharp steps such as the Haar wavelet; the opposite applies to time resolution. Another important consideration is the fast computation of the dilated daughter wavelets. From this point of view, the orthogonal wavelets calculated recursively have more efficient computation than non-orthogonal wavelets. Table1 gives an overview and comparison of commonly used wavelets. Among these wavelets, one of the most widely used mother wavelets suitable for power quality analysis is Daubechies wavelet.

This wavelet is particularly suitable for detecting low amplitude, short duration,fast decaying and oscillating type of signals,encountered frequently in power systems [12,13].

2.1. Multiresolution Analysis of the DWT

Multiresolution analysis is the most important concept for constructing scaling functions and wavelets. A signal, in the Multiresolution analysis, is

viewed at various levels of resolutions [14,15]. By the multiresolution analysis, this signal is first divided into slowly varying and rapidly varying segments through the discretization of the signal using a step size of two. Then, the slowly varying segment is discretized again to form next-level segments. After performing several discretizations, the signal can be decomposed into a series of detail segments and one approximation segment. These discretizations are also termed the decomposition of a signal. Figure 1 illustrates the one-level decomposition and reconstruction of a signal. To understand multiresolution analysis deeply, two-scale relations must be introduced, which relate the scaling function $\varphi(t)$ and the wavelet function $\psi(t)$ at a given scale with the scaling function at the next-higher scale. In other words, $\varphi(t)$ and $\psi(t)$ can be expressed in terms of a series of time-shifted$\varphi(2t)$. The two-scale relations can be written as

$$\phi(t)=\sum_k L_R(k)\phi(2t-k) \tag{1}$$

$$\psi(t)=\sum_k H_R(k)\phi(2t-k) \tag{2}$$

where $L_R(k)$ and $H_R(k)$ are two sequences, which are the coefficients of lowpass and highpass filters for reconstructing the decomposed signal respectively. To determine $L_R(k)$, Daubechies [16,17] considered the z-transform of $L_R(k)$ as the following equation.

$$\overline{L_R}(z)=(\frac{1+z}{2})^m \bar{s}(z) \tag{3}$$

where $\overline{L_R}(z)$ is the z-transform of the sequence $L_R(k)$ and m is the order of Daubechies scaling function. To find $\bar{s}(z)$ is the main task in solving equation (3). Since $\overline{L_R}(z)$ must satisfy the orthogonality property, there exists the following relation.

$$\left|\overline{L_R}(z)\right|^2+\left|\overline{L_R}(-z)\right|^2=1 \tag{4}$$

where $z=e^{-jw/2}$. Substituting Euler identity equation and equation (3) into (4) gets

$$\cos^{2m}\frac{w}{4}\left|\bar{s}(z)\right|^2+\sin^{2m}\frac{w}{4}\left|\bar{s}(-z)\right|^2=1 \tag{5}$$

Then, solving (5) for $\left|\bar{s}(z)\right|^2$ would obtain:

$$\left|\bar{s}(z)\right|^2=\sum_{k=0}^{m-1}\binom{m+k-1}{k}\sin^{2k}\frac{w}{4} \tag{6}$$

$$\text{or}\quad \left|\bar{s}(z)\right|^2=\frac{a_0}{2}+\sum_{k=1}^{m-1}\cos\frac{kw}{2} \tag{7}$$

where

$$a_k=(-1)^k\sum_{n=0}^{m-k-1}\frac{1}{2^{2(k+n)-1}}\binom{2(k+n)}{n}\binom{m+k+n-1}{k+n} \tag{8}$$

By applying Riesz's lemma to (7), $\bar{s}(z)$ is determined and given as:

$$\bar{s}(z)=Q\prod_{g=1}^{G}(z-r_g)\prod_{h=1}^{H}(z-z_h)(z-z_h^*),\quad G+2H=m-1 \tag{9}$$

where $\{r_g\}$ are the nonzero real roots, $\{z_h\}$ are the complex roots of $z^{m-1}\left|\bar{s}(z)\right|^2$ inside a unit circle, $\{z_h^*\}$ are the conjugate of $\{z_h\}$, and Q is a constant such that $\bar{s}(1)=1$ [2, 18]. Once $\bar{s}(z)$ is determined, the sequence of $L_R(k)$ can be determined by substituting $\bar{s}(z)$ into (3), expanding the substitution result, then extracting the coefficients from the expanded polynomial equation. Finally, the other three filters, i.e. $H_R(k)$, $L_D(k)$, and $H_D(k)$, can be found easily by just changing the order and sign of the sequence of $L_R(k)$.

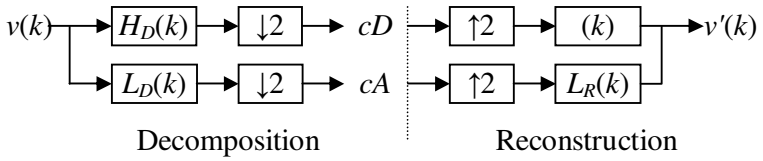

Fig. 1 The structure of signal decomposition and reconstruction

An example of numerical calculation for m=3 is shown in the following section.

2.2. Calculation of the Filter Coefficients

A numerical calculation of the filter coefficients for Daubechies wavelet with order 3 (Daub3) is demonstrated in this section. By considering (7) with m = 3, the values of [a_0, a_1, a_2] can be determined, i.e. [a_0, a_1, a_2]=[19/2, -9/2, 3/4], which gives

$$\left|\bar{s}(z)\right|^2 = \frac{19}{4} - \frac{9}{2}\cos\frac{w}{2} + \frac{3}{4}\cos w \tag{10}$$

Substituting

$$\cos\frac{w}{2} = \frac{z + z^{-1}}{2} \quad and \quad \cos w = \frac{z^2 + z^{-2}}{2} \tag{11}$$

into (10) and multiplying z^2 on both sides would obtain

$$z^2\left|\bar{s}(z)\right|^2 = \frac{1}{8}(3z^4 - 18z^3 + 38z^2 - 18z + 3) \tag{12}$$

The roots of (12) show no real roots but four complex roots, whichare [0.2873-0.1529i, 0.2873-1.4439i, 2.7127+1.4439i, 2.7127+0.1529i]. However, only the first complex root is inside the unit circle. Thus, we can simplify (9) as

$$\bar{s}(z) = Q(z - z_1)(z - z_1^*) \tag{13}$$

where z_1 = 0.2873-0.1529i, z_1^* = 0.2873+0.1529i, and Q = 1.8822. Plugging (13) to (3), we get

$$\begin{aligned}\overline{L_R}(z) = {} & 0.0249 - 0.0604z - 0.0955z^2 + 0.3252z^3 \\ & + 0.5706z^4 + 0.2353z^5\end{aligned} \tag{14}$$

The coefficients of (14) are the sequence of $L_R(k)|_{k=0\text{-}5}$. By repeating these steps described above, the two-scale sequence $L_R(k)$ for Daub2, Daub3, and Daub4 scaling functions are given in Table 2.

Table 2. Sequence of $L_R(k)$ for Daubechies scaling function

	Daub2 m=2	Daub3 m=3	Daub4 m=4
k	$L_R(k)\|_{k=0\text{-}3}$	$L_R(k)\|_{k=0\text{-}5}$	$L_R(k)\|_{k=0\text{-}7}$
0	-0.0915	0.0249	-0.0075
1	0.1585	-0.0604	0.0233
2	0.5915	-0.0955	0.0218
3	0.3415	0.3252	-0.1322
4		0.5706	-0.0198
5		0.2353	0.4461
6			0.5055
7			0.1629

As mentioned previously, the sequence $L_R(k)$ are coefficients of the low pass filter for reconstruction of the decomposed signal. If we reverse the order of this sequence, and then multiply every even element by -1, we obtain the high pass filter coefficients, i.e. $H_R(k)$, for reconstruction. Furthermore, the low pass and high pass filter coefficients for decomposition, i.e. $L_D(k)$ and $H_D(k)$, could be determined by reversing the order of the sequences of $L_R(k)$ and $H_R(k)$ respectively.

3. Design of the DWT Filter Banks

The DWT can be realized using a multi-stage filter with the mother wavelet function as the low pass filter $L_D(k)$ and the scaling function as the high pass filter $H_D(k)$. The high pass and low pass filters are not independent of each other, but are related by

$$H_D(K - 1 - k) = (-1)^k L_D(k) \tag{15}$$

where K is the filter length or the number of filter coefficients. Filters satisfying this condition are commonly applied to signal processing and termed "quadrature mirror filters"[12].

The output of the high pass filter gives the detailed

version of the high-frequency component of the signal. In contrast, the low pass filter provides the approximate version of the low-frequency component, which is then further split to go through other high pass and low pass filters to obtain the next level of the detail and approximation versions. By conducting this process, the DWT can be implemented.

If the original signal is sampled at f_s Hz, then the highest frequency that the sampled signal could faithfully represent is $f_s/2$ Hz. Therefore, the first detail version would cover the band of frequencies between $f_s/2$ and $f_s/4$ Hz. Thus, the first approximation version would include the rest of bandwidth [0, $f_s/4$] Hz. In the next level, the second detail would capture the band of frequencies between $f_s/4$ and $f_s/8$ Hz, and the third detail would cover the band of frequencies between $f_s/8$ and $f_s/16$ Hz as shown in figure 2. Namely, the bandwidth of the detail version in the i_{th}-level can be expressed as [$f_s/(2^{i+1})$, $f_s/(2^i)$]. In the experiment, f_s is set at 8000Hz, thus decomposing it three-times would divide the band into [0, 500, 1000, 2000, 4000] Hz. The maximum level that an N-point signal can be decomposed relies on the number of signal points and the order of Daubechies wavelets used for DWT. This relationship is expressed as

$$L_{\max} = \log_2 N - \log_2 2m \tag{16}$$

where m is the order of used Daubechies wavelets.

Since the process of down-sampling by two follows the convolution in each decomposition level, $\log_2 N$ represents the times that an N-point signal can be decimated by two.

However, the length of decimated signal must be longer than the length of filter coefficients to ensure a meaningful convolution. Therefore, the length of filter coefficients,i.e.$2m$,must be considered in this equation.

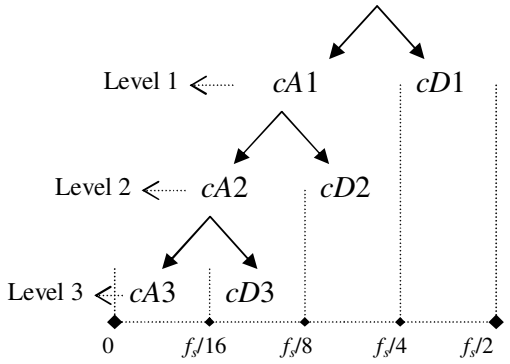

Fig. 2. Bandwidth division of the DWT

4. Implementation of the Decomposition Algorithm

In the first-level decomposition, the sequences $L_D(k)$ and $H_D(k)$ are utilized to convolve with the original signal $v(k)$ to realize the low/high pass filtering process. The convolution result is then followed by decimation by a factor of two. The convolution and decimation can be combined and expressed mathematically as

$$\begin{aligned} cA1(k) &= \{L_D(k) * v(k)\} \downarrow 2 \\ &= \{\sum_k L_D(k-n)\cdot v(n)\} \downarrow 2 \\ &= \sum_k L_D(2k-n)\cdot v(n) \end{aligned} \tag{17}$$

$$cD1(k) = \sum_k H_D(2k-n)\cdot v(n) \tag{18}$$

where $cA1(k)/cD1(k)$ are the approximation/detail coefficients of discrete wavelet transformation results of the 1st-level decomposition. Since the decimation would disregard every even point of the convolved sequence, the calculation of convolution is conducted by shifting the coefficients of filters with step size of two for each inner product such that the calculation load can be cut in half. Such a modification can remove the redundant calculation, thus saving time for other processes.

For the DSP implementation purpose, the code programming for this modified convolution is given as the following matrix multiplication.

For the 2nd-level decomposition, the approximation coefficients $cA1(k)|_{k=1\text{-}512}$ are convolved again with the low/high pass filter coefficients. Consequently, the 2nd-level approximation and detail coefficients (i.e. $cA2(k)|_{k=1\text{-}256}$ and $cD2(k)|_{k=1\text{-}256}$) are obtained.

$$\begin{bmatrix} H_D(1) & H_D(2) & H_D(3) & H_D(4) & 0 & 0 & \cdots & \cdots & \cdots \\ 0 & 0 & H_D(1) & H_D(2) & H_D(3) & H_D(4) & 0 & \cdots & \cdots \\ 0 & 0 & 0 & 0 & H_D(1) & H_D(2) & H_D(3) & H_D(4) & \cdots \\ \vdots & \vdots & \vdots & \vdots & \vdots & \vdots & \vdots & \vdots & \vdots \end{bmatrix} \begin{bmatrix} v(1) \\ v(2) \\ \vdots \\ v(1024) \\ 0 \\ 0 \end{bmatrix} = \begin{bmatrix} cD1(1) \\ cD1(2) \\ \vdots \\ cD1(512) \end{bmatrix} \tag{19}$$

$$\begin{bmatrix} L_D(1) & L_D(2) & L_D(3) & L_D(4) & 0 & 0 & \cdots & \cdots & \cdots \\ 0 & 0 & L_D(1) & L_D(2) & L_D(3) & L_D(4) & 0 & \cdots & \cdots \\ 0 & 0 & 0 & 0 & L_D(1) & L_D(2) & L_D(3) & L_D(4) & \cdots \\ \vdots & \vdots & \vdots & \vdots & \vdots & \vdots & \vdots & \vdots & \vdots \end{bmatrix} \begin{bmatrix} v(1) \\ v(2) \\ \vdots \\ v(1024) \\ 0 \\ 0 \end{bmatrix} = \begin{bmatrix} cA1(1) \\ cA1(2) \\ \vdots \\ cA1(512) \end{bmatrix} \tag{20}$$

5. Experimental Setup

Numerical works of power quality analysis by wavelet transform were implemented on a PC so that the complex calculation of wavelet transform could be realized easily.

However, the product of this implementation is not portable and the cost is considerable. In this study, a high-performance, low-cost, and floating-point DSP chip TMS320C6711 mounted on the TMS320C6711 DSK board is utilized as the core of the hardware implementation. It features eight 32-bit instructions per cycle, 150 MHz clock rates, and 900 MFLOPS, and is very suitable for realization of the instrument.

5.1. Hardware structure

The power voltage signal prior to the analog-to-digital conversion (ADC) must be lowered to an acceptable level for ADC by a potential transform (PT), and the current is also converted to an appropriate voltage signal by a current transform (CT). In order to produce the controllable power disturbances, an arbitrary function generator is utilized in this study to directly generate the power disturbances, such as voltage sag, swell, and interrupt. A number of real power disturbance waveforms captured from a power plant are coded on a PC and then sent to the arbitrary function generator through a GPIB interface to output the simulated power quality events. The experimental setup is shown in figure 3.

5.2. Software structure

The algorithm presented as a flow chart for the power disturbance analysis using DWT is shown in figure 4. The power signal is first converted to a digital format and then put through the power quality event detection. The detection is conducted by comparing the sampled signal $v(k)$ with a perfect sinusoidal waveform $d(k)$ point by point. If the difference between both exceeds a threshold value e_T, the system starts the analysis of DWT on this captured power quality event.

Since this system is implemented on a DSP board and the memory space is limited, the DWT analysis is launched only at the occurrence of power disturbances. Such implementation could reduce the total required computation and realize real-time analysis. The purpose of DWT initialization is to configure the levels to be decomposed and the order of Daubechies wavelet. The DWT would decompose the power disturbance signal based on these configurations. The whole algorithm shown in figure 4 is coded in C language associating some assembly-language subroutines.

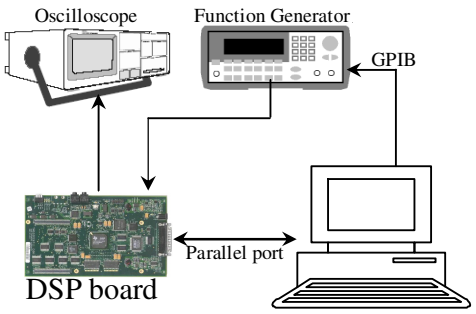

Fig. 3. The hardware structure of experimental setup

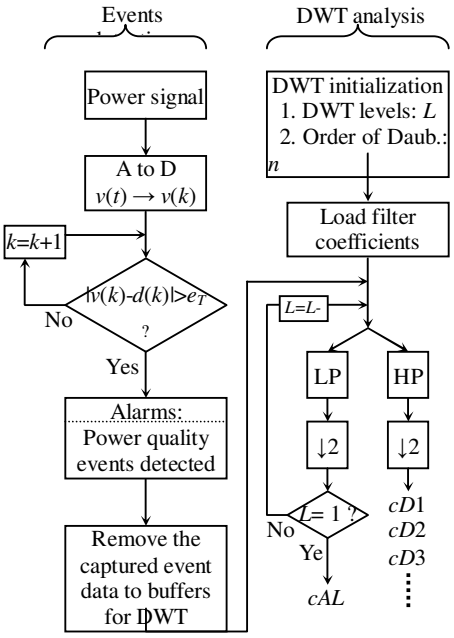

Fig. 4 The flow chart of the software structure

6. Experimental Results

6.1. Determination of Occurrence Time for Power Disturbances

Wavelet transform provides an excellent time localization feature when a transient or high-frequency disturbance occurs in a normal signal. In order to calculate the occurrence time of disturbance, the system searches for the impulses in the decomposed level *cD*1, *cD*2, and *cD*3, in which the impulses location means the point that the disturbance appears. The DSP stores the clock time every 1024 sample points, denoted as T_n. If the disturbance occurs in the k_{th} point at the level of *cDi* (*i*=1,2,3…), then the occurrence time can be calculated by

$$T_d = T_n + \frac{(k-1)2^i + 1}{8000} \tag{21}$$

where 8000 is the sampling rate (Hz). For example, figure 5 illustrates a power interrupt signal and its DWT results in the *cD*1 level. The impulse in the *cD*1 level appears at the 369_{th} point, and T_n is stored as 9.088 seconds which is counted from the time at which the system turned on. Therefore, the occurrence time is determined as 9.088+ ((369-1)×2^1+1)/8000 = 9.180 seconds.

6.2. Decomposition Results of Power Disturbances

A number of power disturbances have been analyzed by the DWT implemented in the DSP board, such as perfect sine waveform, power sag, swell, interrupt, and oscillation transient. All of these experimental results show that the proposed DWT implementation is able to decompose these disturbance waveforms into several frequency bands. The disturbance occurrence time can be immediately localized in the corresponding bands.

One of the tested waveforms is presented here for demonstration. It is a power sag, whose decomposition result is displayed in figure 6. In this figure, subplot (a) is the original waveform of the power sag, (b) is the *cD*1 which is the coefficients of the detail version in level 1 covering [2000-4000] Hz, (c) is the *cD*2 covering [1000-2000] Hz, (d) is the *cD*3 covering [500-1000] Hz, and (e) is the *cA*3 which is the coefficients of the approximation version in level 3, covering [0-500] Hz. The disturbances in this power sag waveform are pointed out by large-magnitude impulses in each band. The highest frequency band *cD*1 shows the most precise time-localization ability among these four bands due to the best frequency resolution of this band.

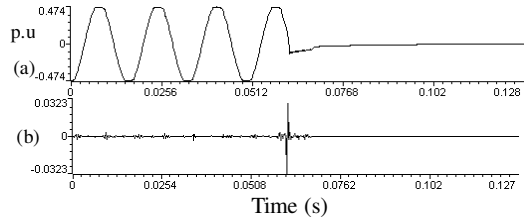

Fig. 5. (a) The interrupt signal and (b) its first level of decomposition result *cD*1

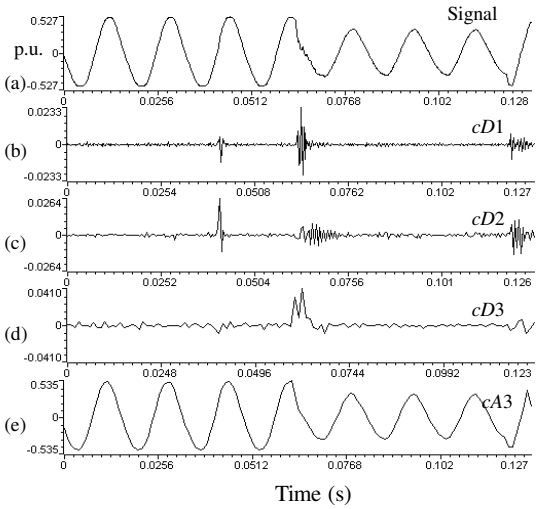

Fig. 6. The power sag waveform and its decomposition results

7. Discussions

7.1. Frequency Response of Filers

An ideal filter, with the low-pass filter for example, completely eliminates all frequencies above the cut-off frequency (half-power point) while passing those below unchanged. The frequency response curve of the ideal filter displays a vertical sharpness at the cut-off frequency. An ideal low-pass filter can be realized theoretically by multiplying a signal by the rectangular function in the frequency domain or, equivalently, by convolution with a sinc function in the time domain. However, it is not realizable for a practical and finite-length signal because the sinc function extends to infinity, termed the infinite impulse response (IIR) filter. In addition, the realization of an ideal filter, with infinite-length coefficients, would require much more computation than a practical filter. In contrast, the DWT employs the finite impulse response (FIR) and orthogonal filter to avoid redundant computation, although at the cost of filter leakage.

For Daubechies wavelets, the scaling functions and wavelets along with their magnitude spectrum obtained from the Fourier transform are shown in figure 7.

Figure 7(a) shows that both high-pass and low-pass filters of the first-level decomposition have a cut-off frequency of 2000 Hz at which the magnitude is 0.707 p.u. (i.e. $1/\sqrt{2}$). Therefore, the frequency band of [0, 4000] Hz is split into [0, 2000] and [2000, 4000] Hz. The filtered and decimated signal in the band of [0, 2000] Hz is then decomposed again and separated into [0, 1000] and [1000, 2000] Hz by the filters that have the frequency response shown in figure 7(b). Similarly, the band of [0, 1000] Hz is further divided into [0, 500] and [500, 1000] Hz in the third-level of decomposition. In figure 7(b), the frequency response curves on the right side exhibit the 3-dB bandwidth of 1000 Hz. The 3-dB bandwidth is defined as the difference between the two frequencies on either side of the peak at which the squared magnitude of the frequency response is exactly half its peak value. This 3-dB bandwidth is centered at 1500 Hz and covers the band from 1000 to 2000 Hz. This provides a Q-factor, determined by the ratio of the center frequency to the 3-dB bandwidth, of roughly 0.67 for this band pass filter. The Q-factor maintains consistency with respect to the wavelet and scaling function dilation because

$$F[\psi(t/a)] = |a|\Psi(aw) \tag{22}$$

$$F[\phi(t/a)] = |a|\Phi(aw) \tag{23}$$

where $F[\ ]$ represents Fourier transform and $\Psi(\ )/\Phi(\ )$ denote the Fourier transform of $\psi(\ )/\varphi(\ )$ respectively. The center frequency of $F[\psi(t/a)]$ for any

a is at 1/|*a*| times the center frequency of the mother wavelet, and its 3-dB bandwidth is also 1/|*a*| times the 3-dB bandwidth of the mother wavelet. Consequently, the ratio of the center frequency to the 3-dB bandwidth yields the same value for the *Q*- factor as before [19]. Thus, the filtering process for each level of decomposition actually applies a set of constant-*Q*-factor band pass filters, which is also the natural characteristic in dilating the wavelet or scaling function for wavelet transformation.

7.2. Filter Leakage

One issue raised by the FIR filter is filter leakage. When a signal falls within a filter, it will also appear at a reduced level in the adjacent filters. This would cause the energy of a signal in a certain filter band to leak into another band, consequently causing possible fault diagnosis of energy distribution. To illustrate the filter leakage, a harmonic distorted signal consisting of the fundamental 60 Hz and its 3rd, 5th, and 7th harmonic components, those all falling inside the band of [0, 500] Hz, is generated and decomposed by using Daub2 (filter length: 4) and Daub8 wavelets (filter length: 16) separately. The decomposition results are shown in figures 8 and 9 respectively. Because these harmonics belong to the band of [0, 500] Hz (*cA*3 band), the rest of the bands ideally should not display any energy relating to these harmonics. However, it is seen that a certain amount of harmonics energy leaks to higher-frequency bands *cD*3 and *cD*2, even the highest one *cD*1 shown in figure 8. Since a longer-length filter would cause less energy leakage. The decomposition result by utilizing Daub8 wavelet, with a longer filter length than Daub2, has the leakage appearing in the band of *cD*3 only and none in *cD*2 and *cD*1, as shown in figure 9. The easiest way to reduce filter leakage is to compute with a longer-length filter, yet at the expense of taking larger time sequences for the process.

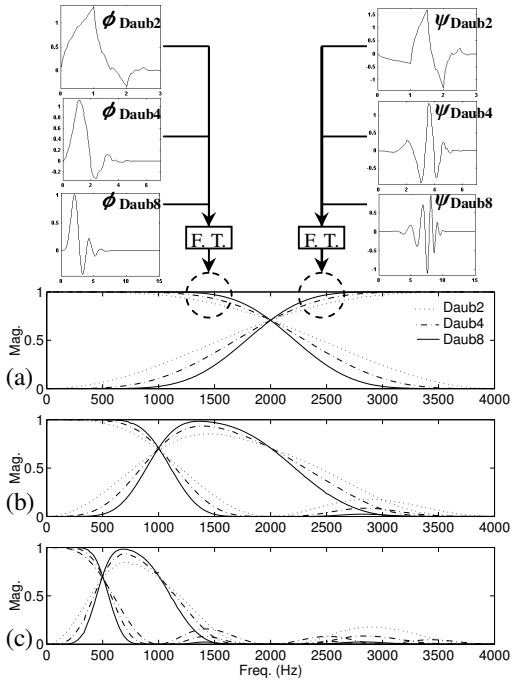

Fig. 7. Daubechies wavelets and their scaling functions along with Fourier Transform results.

7.3. Calculation Time of the DWT

As to the hardware implementation aspect, the time consumption of the DWT is an important issue. Less time consumption would increase the possibility of realizing real-time analysis. The DWT is basically a convolution of the signal and filter coefficients. The convolution in discrete format can be done mathematically by an inner-product that can be implemented easily by the instruction of Multiplication-Accumulation (MAC) in most of the DSP chips. The MAC instruction can complete one multiplication and addition in one clock cycle. In the experiment, the Daubechies wavelet is applied to analyze the signal. The order of Daubechies wavelet is denoted by *m*. A *L*-level decomposition on a *N*-point signal would cost a period of time:

$$T_{DWT} = 2 \cdot N \cdot m \cdot (2 - \frac{1}{2^{L-1}}) \cdot T_{MAC} \quad (24)$$

where T_{MAC} signifies the time consumed by one MAC instruction. This equation indicates that the time consumption for a DWT is proportional to the signal

length and the order of Daubechies wavelets. In order to maintain both limited filter leakage and less calculation time, the DSP implementation, therefore, in this study takes Daub4 for the wavelet transform.

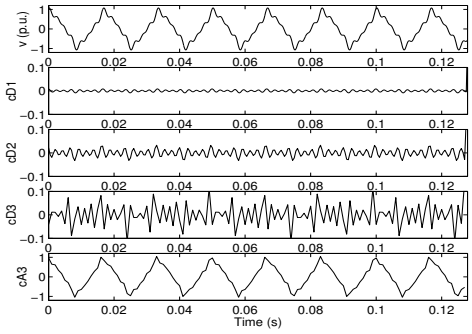

Fig. 8. DWT analysis of the harmonic waveform by using Daub2 wavelet.

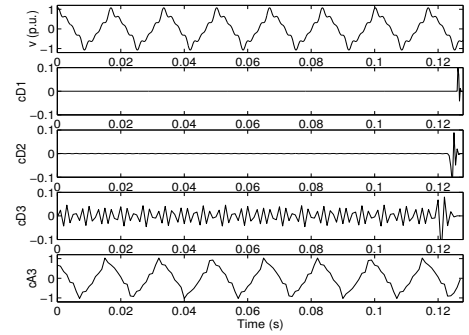

Fig. 9. DWT analysis of the harmonic waveform by using Daub8 wavelet.

8. Conclusions

In this paper, a new DWT based power disturbance analysis scheme has been described. The algorithm is implemented with a Texas Instruments (TI) 32-bit TMS320C6711 DSP along with TLC320AD535 16-bit analog to digital converter. The investigation reveals that the proposed method can successfully be employed for real-time analysis of power disturbances, such as the frequency-time decomposition, detection of disturbances, and transient localization.

The developed scheme is highly reliable and flexible to suit the requirements of various power disturbances. Unlike a PC-based implementation, this DSP-based prototype has a simple structure and small dimensions. It has the potential to be the basis for hand-held devices of power disturbance analyzers.

References:

[1] Driesen ,J.L. and Bel,ams, R.J.M.:"Wavelet-based power quantificatiom approaches ",IEEE Transactions on Instrumentation and Measurement, Vol.52, Issue 4,Aug.2003, pp. 1232-1238.

[2] C. K. Chiu, Wavelets: A Mathematical Tool for Signal Analysis. Philadelphia: SIAM, 1997.

[3] Littler, T.B. and Morrow, D.J.: "Wavelets for the analysis and compression of power system disturbances", IEEE Transactions on Power Delivery, Vol.14, Issue 2, April 1999 pp. 358 – 364.

[4]Daubechies, I.: "The wavelet transform, time-frequency localization and signal analysis", IEEE Transactions on Information Theory,Vol.36, Issue 5, Sept. 1990 pp.961 – 1005.

[5] He, H. and Starzyk, J.A.: "A Self-Organizing Learning Array System for Power Quality Classification Based on Wavelet Transform", IEEE Transactions on Power Delivery, Vol.21, Issue 1, Jan. 2006 pp.286 – 295.

[6] Wilkinson, W.A. and Cox, M.D.: "Discrete wavelet analysis of power system transients", IEEE Transactions on Power Systems, Vol.11, Issue 4, Nov. 1996 pp.2038 – 2044

[7] Galli, A.W. and Nielsen, O.M.: "Wavelet analysis for power system transients", IEEE Computer Applications in Power, Vol.12, Issue 1, Jan. 1999, pp.:16, 18, 20, 22, 24 - 25

[8] Zwe-Lee Gaing: "Wavelet-based neural network for power disturbance recognition and classification", IEEE Transactions on Power Delivery, Vol.19, Issue 4, Oct. 2004 pp.1560 – 1568.

[9] T.X. Zhu, S.K. Tso, and K.L Lo: "Wavelet-based

fuzzy reasoning approach to power-quality disturbance recognition", IEEE Transactions on Power Delivery Vol.19, Issue 4, Oct. 2004, pp.1928 – 1935.

[10] Shyh-Jier Huang, Tsai-Ming Yang, and Jiann-Tseng Huang: "FPGA realization of wavelet transform for detection of electric power system disturbances", IEEE Transactions on Power Delivery, Vol. 17, Issue 2, April 2002, pp.388 - 394

[11] Arghya Sarkar and S. Sengupta: "A novel instantaneous power factor measurement method based on wavelet transform", IEEE Power India Conference,10-12 April 2006.

[12] Chul Hwan Kim and Raj Aggarwal: "Wavelet transforms in power systems. I. General introduction to the wavelet transforms", Power Engineering Journal, Vol.14, Issue 2, April 2000 pp.81 – 87.

[13] Martin Vetterli and Cormac Herley: "Wavelets and filter banks: theory and design", IEEE Transactions on Signal Porcessing, Vol.40, No. 9, September 1992, pp. 2207-2232

[14] Y. Meyer, Wavelets: Algorithms and Applications. Philadelphia:SIAM, 1993.

[15] S. Mallat: "A theory of multiresolution signal decomposition: the wavelet representation," IEEE Transactions on Pattern Anal. Machine Intell., 11, 1989 pp. 674-693

[16] I. Daubechies: Ten Lectures on Wavelets. Philadelphia: SIAM, 1992.

[17] I. Daubechies: "Orthonormal bases of compactly supported wavelets," Communication Pure Application Mathematics, 41. 1988 pp. 909-996

[18] Jaideva C. Goswami and Andrew K. Chan, Fundamentals of Wavelets: Theory, Algorithms, and Applications. Wiley-Interscience Publication.

[19] Raghuveer M. Rao and Ajit S. Bopardikar: Wavelet Transforms Introduction to Theory and Applications, Addison Wesley, 1998